Rational Design and Fabrication of ZnO Nanotubes from Nanowire Templates in a Microwave Plasma System

Xian-Hua Zhang, Su-Yuan Xie,* Zhi-Yuan Jiang, Xuan Zhang, Zhong-Qun Tian, Zhao-Xiong Xie, Rong-Bin Huang, and Lan-Sun Zheng

State Key Laboratory for Physical Chemistry of Solid Surfaces, Department of Chemistry, Xiamen University, Xiamen 361005, P. R. China

A nanowire−nanocable−nanotube scheme was designed for fabricating tubular ZnO in a microwave plasma system. Depending on optimal reaction conditions, diameters (from submicrometer to nanometer) and wall thicknesses of the tubular ZnOs can be controlled in the process. Data from morphology analyses, X-ray diffraction, photoluminescence spectra and Raman spectroscopy of the as-prepared ZnO nanotubes support the validity of the proposed three-step route for the fabrication of tubular ZnO.

Introduction

ZnO has been used intensively for its catalytic,[1] electrical,[2] optoelectronic,[3−8] and photoelectrochemical properties.[9] As a kind of versatile material, it is also a potential sensor for NH_3,[10] a photocatalyst to reduce NO_x emission,[11,12] and a wide band-gap (3.37 eV) semiconductor with high binding energy of the exciton ($\sim$60 meV). These promising findings stimulate the interest of scientists to synthesize and assemble a variety of ZnO structures with novel properties, especially those in the nanometer scale, to meet the urgent contemporary requirements in constructing optical and electronic devices toward miniaturization. As a significant advancement of application of ZnO nanomaterials, room-temperature ultraviolet nanowire nanolasers, photodetectors, and optical switches have already been accessed.[13,14]

A number of ZnO nanomaterials with interesting structures and properties have been synthesized, such as nanoparticles,[15] nanorods,[16,17] nanobelts,[18] nanocombs,[19] nanowires,[20,21] tetrapod nanostructures,[22] and a range of novel hierarchical nanostructures with 6-, 4-, and 2-fold symmetries.[23] Besides these nanostructures, one-dimensional (1D) nanotubes have attracted much attention owing to their great potential for fundamental studies and for applications in catalysis, intramolecular junctions, absorption, storage and release systems, etc.[24−27] To our knowledge, however, high-yield synthesis of ZnO nanotubes has rarely been reported in previous investigations. To date, a few groups reported the synthesis of submicrometer tubular ZnO,[28,29] ZnO−Zn coaxial nanocables and ZnO nanotubes.[30,31] However, controlled growth of ZnO nanotubes with expected dimensions and high yield still remains to be investigated.

Rational design and fabrication of nanostructures in desired geometries are important for the urgent demand of constructing nanodevices, and it is fundamentally interesting to develop controllable methods for manufacturing ZnO nanotubes with expected diameters and wall thicknesses. In previous reports, single-crystalline nanowires of Ag_2Se could be synthesized by templating against nanowires of trigonal Se.[32] In that experiment uniform nanowires of trigonal Se were initially synthesized as templates and then allowed to completely react with an aqueous
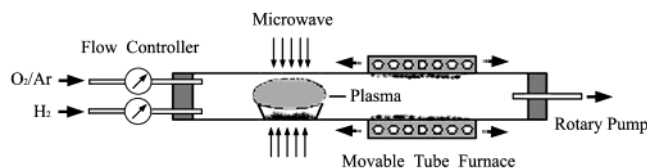

Figure 1. Schematic illustration of microwave plasma system for ZnO nanotubes growth.

$AgNO_3$ solution to form Ag_2Se nanowires at room temperature. On the basis of this illumination, we design a three-step route to manufacture ZnO nanotubes. A microwave plasma system was developed to fabricate ZnO nanotubes with different dimensions in high yield. Interestingly, this microwave plasma method allows the product morphologies to be controlled from Zn nanowires to ZnO nanotubes, and the diameter of the tubular ZnO can be adjusted from submicrometer to nanometer. Additionally, the wall thickness of the ZnO nanotubes can be varied by controlling the oxidation depth of the Zn nanowires.

Experimental Section

Materials. Zn powder and bulk ZnO (analytical grade), H_2 (99.9%), Ar (99.9%), and O_2 (99.9%) are all commercially available.

Synthesis of ZnO Nanostructures. The experimental scheme was shown in Figure 1. Zinc powder was put into a quartz boat placed inside the center of the horizontal quartz tube. As protective gas and carrier gas, pure H_2, was fed into the reaction chamber with appropriate flows (usually, 50 sccm for nanotubes). The pressure in the reactor was maintained at about 4 Torr (with small fluctuation upon gas flow change) by a rotary bump. A 400 W 2.45 MHz microwave source was introduced along a square rectangle wave-conduct pipe to couple the microwave to the quartz tube center for generating stable plasma. The temperature of the microwave plasma was estimated about 1000 °C. A movable tube furnace with 20 cm length was equipped as an assistant heating source. The center temperature of the assistant tube furnace was 700 °C, and the temperature inside the quartz tube was estimated about 500 °C. After reaction for 30 min H_2 flow was stopped, and black Zn product around the inner wall of the quartz tube could be observed. O_2/Ar gas

* Corresponding author. E-mail: syxie@jingxian.xmu.edu.cn.

Design and Fabrication of ZnO Nanotubes

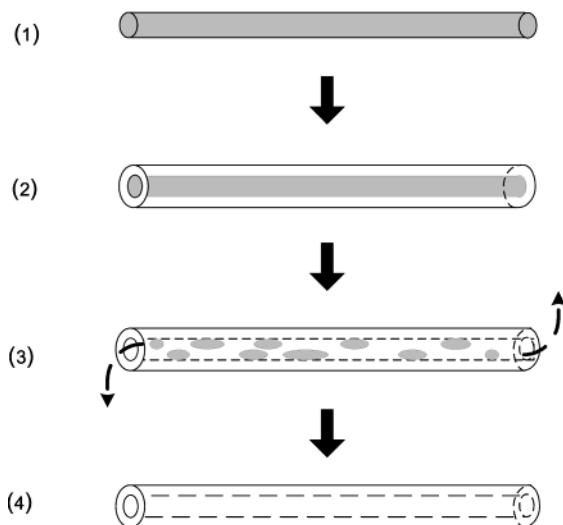*J. Phys. Chem. B, Vol. 107, No. 37, 2003* **10115**

Figure 2. Scheme of ZnO nanotube fabrication from Zn nanowire.

(volume ratio 1:50) was introduced to the microwave plasma system to oxidize the Zn products for 15−30 min. Then, the tube furnace was moved back-and-forth along to the quartz tube until only white powder was left. The as-prepared white products on the inner wall of the quartz tube at the downstream end were collected for characterization.

Characterization. X-ray powder diffraction (XRD) was carried out on a Rigaku DMAX/RC X-ray diffractometer using Cu-kα radiation (λ = 0.154 178 nm). Transmission electron microscopy (TEM) micrographs were taken using a JEM-100CXII transmission electron microscope, while field-emission scanning electron microscopy (FE-SEM) images were taken using a LEO1530 SEM system. High-resolution transmission electron microscopy (HRTEM) images were obtained on a TECNAI F-30 FEG TEM at an acceleration voltage of 300 kV. Raman spectra were acquired with a confocal Raman microscope (LabRam I) excited by a He−Ne laser (632.8 nm). The photoluminescence (PL) spectrum was obtained on a HITACHI F-4500 fluorescence spectrophotometer operated at an exited wavelength of 300 nm and slit (ex/em) of 10.0/10.0 nm, with a Xe lamp as the excitation light source at room temperature.

Results and Discussion

The detailed process of ZnO nanotube manufacture in the microwave plasma system is illustrated as Figure 2, and the scheme of ZnO nanotube growth is described step by step as follows:

(1) Step 1: In the microwave plasma system, Zn nanowires are grown from Zn powders under an H_2 atmosphere inside the quartz tube reactor. Because no catalyst is used in the system, the Zn nanowire growth should be based on a self-catalytic vapor−liquid−solid mechanism. These nanowires act as hard templates to determine the dimensions of final ZnO nanotubes.

(2) Step 2: Low concentration O_2, diluted by inert gas Ar, is introduced into the reaction chamber (quartz tube) for partial oxidation of Zn nanowire, resulting in the formation of Zn−ZnO nanocable, in which Zn is wrapped by ZnO sheath. These Zn−ZnO nanocables will act as the intermediates toward ZnO nanotubes. Accordingly, the oxidation time would affect the wall thickness of the final ZnO nanotubes.

(3) Step 3: A movable tube furnace is mounted outside the quartz tube to maintain an adaptive temperature of about 500 °C inside the quartz tube. This tube furnace is moved over the nanocables back-and-forth. At this temperature condition, the zinc cores of Zn−ZnO nanocables will be depleted slowly due
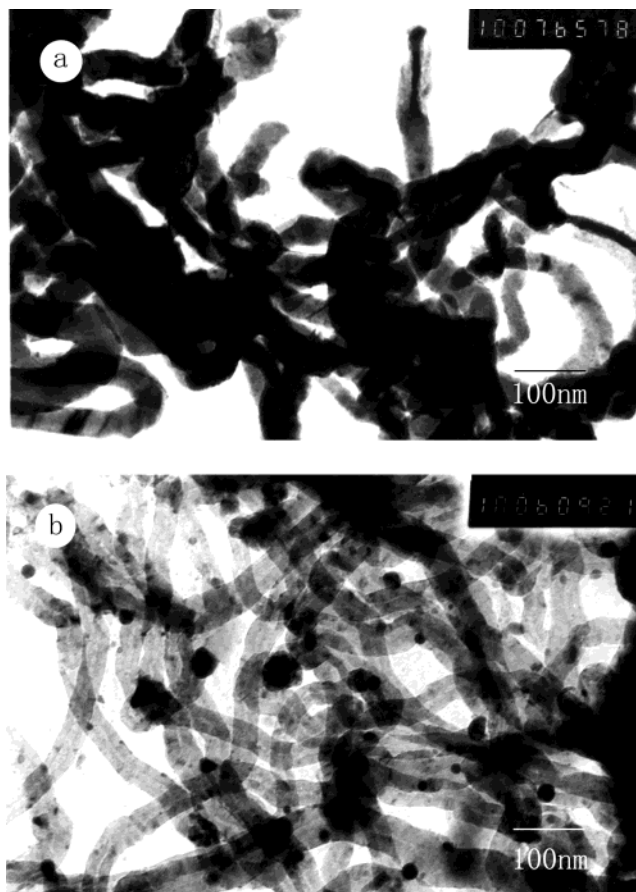

Figure 3. TEM images of (a) Zn−ZnO nanocables and (b) ZnO nanotubes.

to the lower melting point of metal zinc (410 °C) as compared with ZnO (1975 °C). Eventually, the process results in ZnO nanotube after the zinc core is removed completely.

Three-step microwave plasma experiments were carried out according to the designed wire−cable−tube route, and the experimental results demonstrated that various Zn−ZnO nanocables and ZnO nanotubes with different dimensional parameters could be manufactured by adjusting the experimental conditions in step 1−3. If the step 1 was omitted in the experiment, a kind of tetrapod ZnO nanostructure would be produced.[33]

Morphological analyses and X-ray diffraction results strongly support the validity of the proposed strategy for tubular ZnO fabrication. Typical TEM images of the Zn−ZnO nanocables trapped in the reactor before step 3 are given in Figure 3a. Pertinent XRD pattern of the Zn−ZnO nanocables (Figure 4a) confirms that the nanocables are composed of Zn and ZnO (peaks are marked with asterisks), which are ascribed as the core and the sheath of the Zn−ZnO nanocable. Compared with Zn diffraction peaks, the peaks from the ZnO are weak mainly due to the poor crystallinity. Figure 3b shows the morphologies of the final ZnO nanotubes; their XRD pattern (Figure 4b) is indexed as the hexagonal ZnO phase (JCPDS No. 36-1451). These nanotubes bear uniform diameters with outer and inner diameters about 40 and 10 nm, respectively. The average length of the nanotubes is about 1 μm. The yield of ZnO nanotube is high according to the morphology analyses. From the morphology shown in Figure 3, one can find that the outer diameters of the ZnO nanotubes coincide well with the diameters of Zn−ZnO nanocables, demonstrating that the Zn nanowires might act as hard templates, which determined the outer diameter of the ZnO nanotubes.
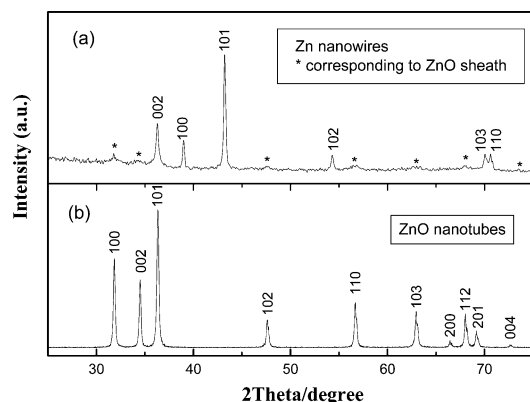
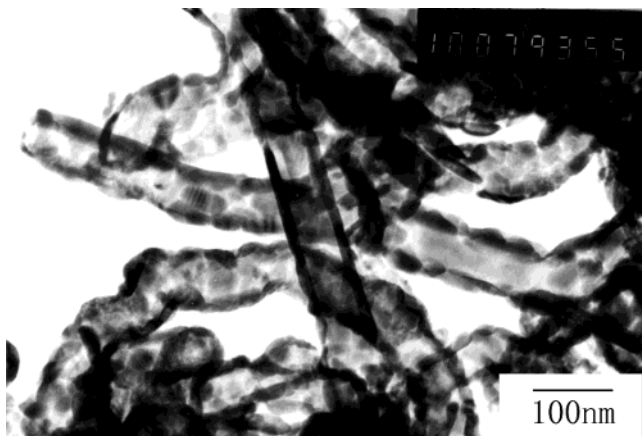**Figure 4.** XRD patterns of (a) Zn−ZnO nanocables and (b) ZnO nanotubes.

Figure 5. TEM image of ZnO nanotubes with thinner walls.

Figure 6. (a) FE-SEM image of tubular ZnOs with submicrometer scale; (b) Magnified FE-SEM image of the end of incomplete tubular ZnOs.

The nanotechnology for controlled manufacture of nanotubes with expected dimensions is of significance for promoting the practical application of this kind of material in nanodevices. For manufacture of ZnO nanotubes with desired wall thickness, the preliminary experiments were carried out with different oxidation times in step 2. As shown in Figure 5, the wall thickness of the as-prepared ZnO nanotube is only about 10 nm if the oxidation time was limited to 15 min. Tubular ZnO with thicker walls were obtained by elongating oxidation time.

On the other hand, the diameter of the tubular ZnO can be adjusted from submicrometer to nanometer by varying the experimental conditions in step 1. In the first step, H_2 acts as both a protective gas and carrier gas, the flow of which will affect the zinc vapor aggregation and Zn wire growth. When H_2 flow was increased to 90 sccm, Zn wires with submicrometer diameters were obtained. As Figure 6a shows, the outer diameters of resulted ZnO tubes are about 200−300 nm, and the average length of the tube is up to 1.5 μm. An FE-SEM image (Figure 6b) was taken for the products obtained in the middle of step 3, in which most of the zinc remains as tubular ZnO and one incompletely hollow end can be seen clearly. When the heating time of the movable tube furnace in step 3 was increased, zinc remaining in the hollow of the ZnO tube would be forced out completely.

Further insight into the ZnO nanotubes can be revealed by HRTEM images. As shown in Figure 7a, the high-resolution image reveals that the ZnO nanotubes have well-crystallized structures. The outer and inner diameters of a chosen ZnO nanotube are about 78 and 18 nm, respectively, and the walls are up to 30 nm in thickness. The magnified image (Figure 7b,
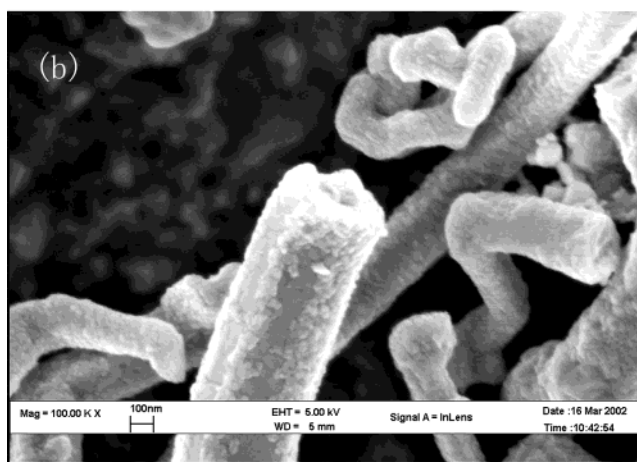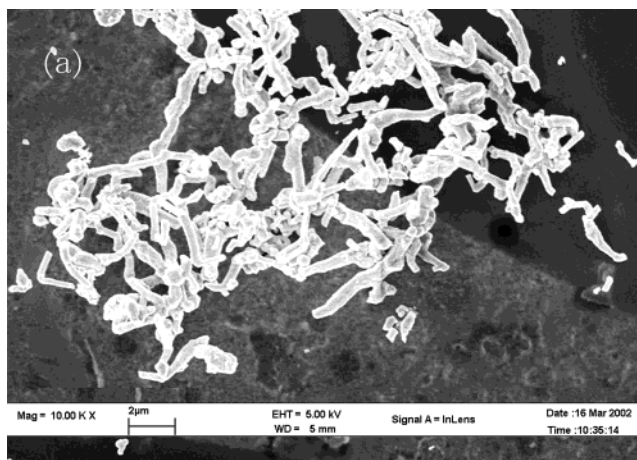
corresponding to the high brightness in Figure 7a) exhibits clear lattice fringes. The fringe spacing ($\sim$0.26 nm) observed in this image agrees well with the space between the [002] lattice planes, reflecting that oxidation of the Zn nanowires is along the [001] direction of hexagonal ZnO. As shown in the high brightness region in Figure 7c and its magnified image in Figure 7d, some defect structures are also found in the ZnO nanotubes. Detailed information of the defect structure is not known yet, but it is speculated that these defects may be correlated with the stress from the zinc core during its exhaustion from the Zn−ZnO nanocable in step 3.

Figure 8 shows that Raman spectra of both the nanotube and the bulk crystal are quite similar, further confirming the product to be pure ZnO nanocrystal. This is also in good agreement with the X-ray diffraction data. ZnO is a Wurtzite-type crystal, which belongs to the space group C_{6v}. The Raman bands at 331, 380, 437, and 576 cm^{-1} are assigned as the E_2, A_1(TO), E_2, and E_1(LO) modes, respectively.[34] It may be necessary to note that a broadening of the asymmetric Raman band at 437 cm^{-1} is observed for ZnO nanotubes in comparison with that of the bulk ZnO. Such a mild difference can be accounted for mainly as the size effect of nanoparticles.[35] The PL spectrum of ZnO nanotubes (Figure 9) reveals two emitting bands, including a strong ultraviolet emission at around 386 nm, and a blue band at about 465 nm. The former band must contribute to the near band edge emission of the wide band-gap ZnO, the latter is not yet clear, which may be in correlation with the defect structures.
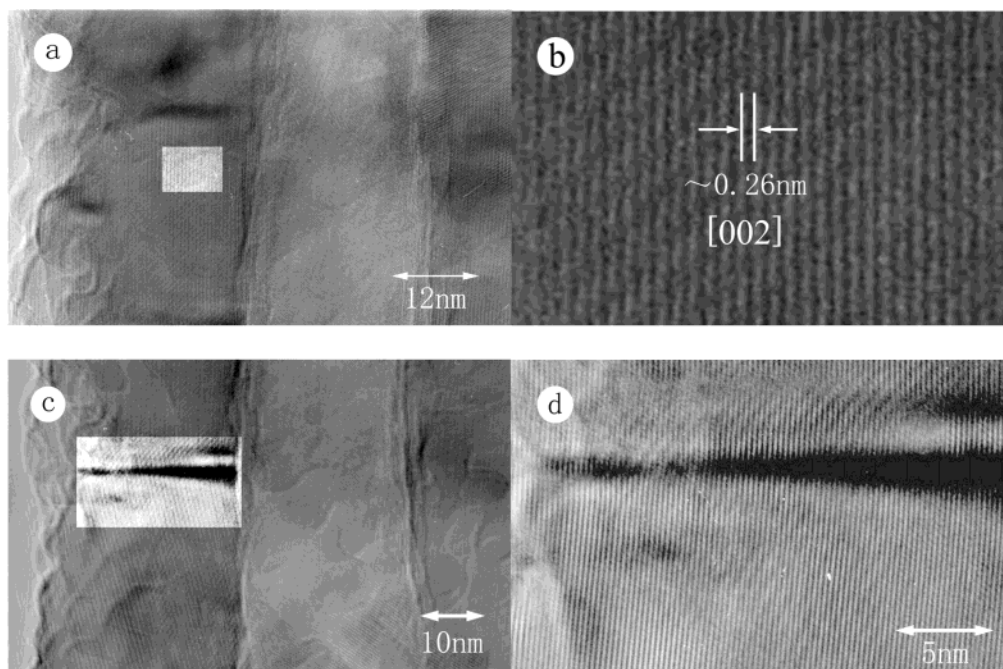
Design and Fabrication of ZnO Nanotubes

J. Phys. Chem. B, Vol. 107, No. 37, 2003 **10117**

Figure 7. HRTEM images of ZnO nanotube: (a) a ZnO nanotube with well-crystallized structure; (b) magnified image corresponding to the high brightness in Figure 7a; (c) a ZnO nanotube with defect structure; (d) magnified image of the defect structure corresponding to the high brightness in Figure 7c.
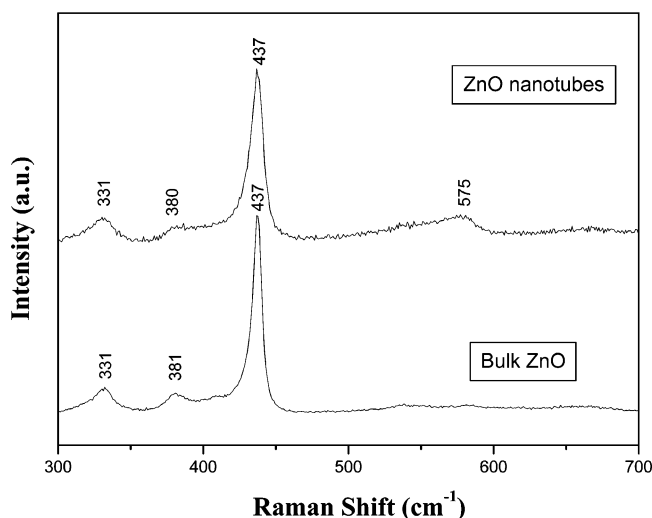

Figure 8. Raman spectra of ZnO nanotubes and bulk ZnO.

Figure 9. Room-temperature PL spectrum of ZnO nanotubes.

Conclusions

In summary, a nanowire−nanocable−nanotube route has been designed to fabricate ZnO nanotubes with desired dimensions in high yield by the microwave plasma method. Zn nanowires grown from Zn powders under a H_2 atmosphere are shown to act as hard templates for constructing Zn/ZnO nanocables via its partial oxidation. The zinc core in the Zn/ZnO nanocables escapes when heated, which eventually leads to complete ZnO nanotubes. Structural parameters of the ZnO nanotube, including diameter and wall thickness, can be rationally adjusted by varying the reaction conditions in the microwave plasma process, such as H_2 flow rate and oxidation time. The diameters of the tubular ZnOs can be adjusted from submicrometer (with outer diameters of about 200−300 nm) to nanometer (outer diameters ranging from 40 to 80 nm), and the walls of the tubular ZnOs varied from 10 to 30 nm in thickness. Morphological analyses, X-ray diffraction, PL spectrum and Raman spectroscopic results support the validity of th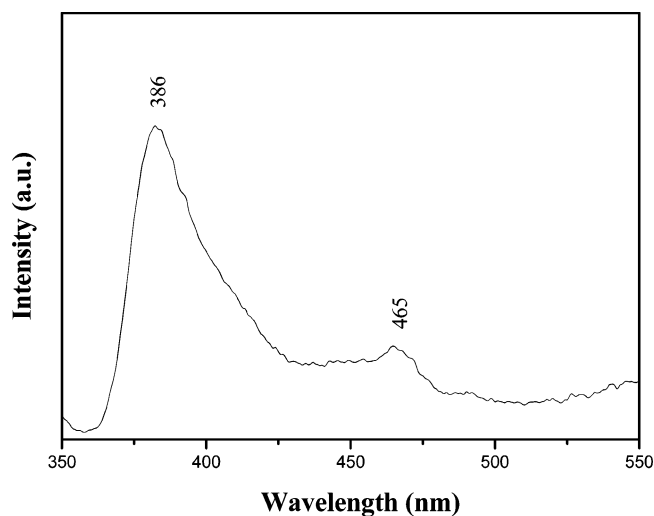e proposed strategy for the fabrication of tubular ZnO. The process may be extended to synthesis of other kinds of nanotubes or nanocables.

References and Notes

(1) King, D. S.; Nix, R. M. *J. Catal.* **1996**, *160*, 76.

(2) Agarwal, G. R.; Speyer, F. *J. Electrochem. Soc.* **1998**, *145*, 2920.

(3) Bagnall, D. M.; Chen, Y. F.; Zhu, Z.; Yao, T.; Koyama, S.; Shen, M. Y.; Goto, T. *Appl. Phys. Lett.* **1997**, *70*, 2230.

(4) Johnson, J. C.; Yan, H. Q.; Schaller, R. D.; Petersen, P. B.; Yang, P. D.; Saykally, R. J. *Nano Lett.* **2002**, *2*, 279.

(5) Sekiguchi, T.; Haga, K.; Inaba, K. *J. Cryst. Growth* **2000**, *214*, 68.

10118 *J. Phys. Chem. B, Vol. 107, No. 37, 2003*

Zhang et al.

(6) Sekiguchi, T.; Miyashita, S.; Obara, K.; Shishido T.; Sakagami, N. *J. Cryst. Growth* **2000**, *214*, 72.

(7) Muthukumar, S.; Zhong, J.; Chen, Y.; Lu, Y.; Siegrist, T. *Appl. Phys. Lett.* **2003**, *82*, 742.

(8) Muthukumar, S.; Emanetoglu, N. W.; Patounakis, G.; Gorla, C. R.; Liang, S.; Lu, Y. *J. Vac. Sci. Technol. A* **2001**, *19*, 1850.

(9) Keis, K.; Vayssieres, L.; Linquist, S. E.; Hagfeldt, A. *J. Electrochem. Soc.* **2001**, *148*, A149.

(10) Sberveglieri, G.; Groppelli, S.; Nelli, P.; Tintinelli, A.; Giunta, G. *Sens. Actuators B* **1995**, *25*, 588.

(11) Rodriguez, J. A.; Jirsak, T.; Dvorak, J.; Sambasivan, S.; Fischer, D. *J. Phys. Chem. B* **2000**, *104*, 319.

(12) Yumoto, H.; Inoue, T.; Li, S. J.; Sako, T.; Nishiyama, K. *Thin Solid Films* **1999**, *345*, 38.

(13) Huang, M. H.; Mao, S.; Feick, H.; Yan, H. Q.; Wu, Y. Y.; Kind, H.; Weber, E.; Russo, R.; Yang, P. D. *Science* **2001**, *292*, 1897.

(14) Kind, H.; Yan, H. Q.; Messer, B.; Law, M.; Yang, P. D. *Adv. Mater.* **2002**, *14*, 158.

(15) Dong, L. F.; Cui, L. Z.; Zhang, Z. K. *Nanostruct. Mater.* **1997**, *8*, 815.

(16) Wu, J. J.; Liu, S. C. *Adv. Mater.* **2002**, *14*, 215.

(17) Pacholski, C.; Kornowski, A.; Weller, H. *Angew. Chem., Int. Ed.* **2002**, *41*, 1188.

(18) Pan, Z. W.; Dai, Z. R.; Wang, Z. L. *Science* **2001**, *291*, 1947.

(19) Yang, P. D.; Yan, H. Q.; Mao, S.; Russo, R.; Johnso, J.; Saykally, R.; Morris, N.; Pham, J. R.; He, R.; Choj, H. J. *Adv. Funct. Mater.* **2002**, *12*, 323.

(20) Zhang, J.; Sun, L. D.; Pan, H. Y.; Liao, C. S.; Yan, C. H. *New J. Chem.* **2002**, *26*, 33.

(21) Kong, Y. C.; Yu, D. P.; Zhang, B.; Fang, W.; Feng, S. Q. *Appl. Phys. Lett.* **2001**, *78*, 407.

(22) Dai, Y.; Zhang, Y.; Li, Q. K.; Nan, C. W. *Chem. Phys. Lett.* **2002**, *358*, 83.

(23) Lao, J. Y.; Wen, J. G.; Ren, Z. F. *Nano Lett.* **2002**, *2*, 1287.

(24) Yao, Z.; Postma, H. W. C.; Balents, L.; Dekker, C. *Nature* **1999**, *402*, 273.

(25) Tremel, W. *Angew. Chem., Int. Ed.* **1999**, *38*, 2175.

(26) Lin, Y.; Rao, A. M.; Sadanadan, B.; Kenik, E. A.; Sun, Y. P. *J. Phys. Chem. B* **2002**, *106*, 1294.

(27) Riggs, J. E.; Walker, D. B.; Carroll, D. L.; Sun, Y. P. *J. Phys. Chem. B* **2000**,*104*, 7071.

(28) Zhang, J.; Sun, L. D.; Liao, C. S.; Yan, C. H. *Chem. Commun.* **2002**, 262.

(29) Vayssieres, L.; Keis, K.; Hagfeldt, A.; Lindquist, S. E. *Chem. Mater.* **2001**, *13*, 4395.

(30) Wu, J. J.; Liu, S. C.; Wu, C. T.; Chen, K. H.; Chen, L. C. *Appl. Phys. Lett.* **2002**, *81*, 1312.

(31) Hu, J. Q.; Li, Q.; Meng, X. M.; Lee, C. S.; Lee, S. T. *Chem. Mater.* **2003**, *15*, 305.

(32) Gates, B.; Wu, Y. Y.; Yin, Y. D.; Yang, P. D.; Xia, Y. N. *J. Am. Chem. Soc.* **2001**, *123*, 11500.

(33) Zhang, X. H.; Xie, S. Y.; Jiang, Z. Y.; Xie, Z. X.; Huang, R. B.; Zheng, L. S.; Kang, J. Y.; Sekiguchi, T. *J. Solid State Chem.* **2003**, *173*, 109.

(34) Rajalakshmi, M.; Arora, A. K.; Bendre, B.S.; Mahamuni, S. *J. Appl. Phys.* **2000**, *87*, 2445.

(35) Li, B. B.; Yu, D. P.; Zhang, S. L. *Phys. Rev. B* **1999**, *59*, 1645.